Petroleum Science 23 (2026) 5870–5886

Contents lists available at ScienceDirect

Petroleum Science

journal homepage: www.keaipublishing.com/en/journals/petroleum-science

Original Paper

Techno-economic feasibility evaluation framework for reverse-flow retrofitting in multi -product pipelines aimed at benefit augmentation

Ming-Yue Huang [a], Ren-Fu Tu [a], Qi Liao [a,*], Xiao-Meng Bai [a], Zheng-Bing Li [b], You-Yi Liang [c], Si-Ya Cai [c], Yong-Tu Liang [a,d]

[a] Beijing Key Laboratory of Urban Oil and Gas Distribution Technology, China University of Petroleum (Beijing), Beijing, 102249, China
[b] PipeChina Institute of Science and Technology, Tianjin, 300450, China
[c] PipeChina Oil & Gas Control Center, Beijing, 100013, China
[d] Interdisciplinary Centre for Green and Intelligent Pipeline Transportation, Beijing University of Chemical Technology, Beijing, 100029, China

A R T I C L E I N F O

Article history:
Received 25 October 2025
Received in revised form
9 March 2026
Accepted 22 May 2026
Available online 28 May 2026

Edited by Xi Zhang

Keywords:
Reverse-flow
Transport capacity
Economic evaluation framework
Multi-modal control strategies
Pipe diameter correction

A B S T R A C T

As China's energy transition advances, optimizing flow direction in multi-product pipelines becomes critical to accommodate structural shifts in oil consumption, particularly reverse-flow operations. Normally, pipelines adopt a large-to-small diameter design to match declining flowrates, but reverse-flow disrupts this arrangement, leading to a substantial drop in transport capacity, the reconstruction of pressure and contamination control strategies. Therefore, this paper proposes an economic evaluation framework for the reverse-flow multi-product pipelines. Based on pipeline flowrate constraints, a model is constructed, with a flowrate interval expansion factor introduced to retrofit pipe segments and enhance reverse-flow capacity. Within the model, the nonlinear flowrate-pipe diameter relationship is addressed via piecewise linearization, while a correction method minimizes approximation errors. Taking a pipeline as a case study, the sensitivity analysis of factors impacting the economic performance of renovation project is conducted. The results show, i) minor renovations increase transport capacity of reverse-flow by 39% measured by total turnover volume. ii) The net benefit of renovation project is most sensitive to unit price of pipeline transportation, which the investment becomes viable when unit price of pipeline transportation exceeds 0.1755 CNY/(t·km). iii) Compared with the normal rule, the proposed framework increases transportation revenue by 19.97%–20.29%. iv) Compared with the pre-renovation condition, the potential for economic benefit growth ranging from approximately 27.93% to 31.21%. v) When model parameters such as flowrate interval expansion factor and economic velocity fall within reasonable ranges, the renovation scheme is valid. This study optimizes reverse-flow capacity through multi-modal control strategies and corrects the diameter of pipe segments, enhancing operational flexibility and efficiency in pipeline networks and providing a cost-optimized renovation solution for pipe segments. Future studies should prioritize real-time updating and feedback mechanisms for pipeline capacity during flow-direction optimization.

1. Introduction

1.1. Background

Against the backdrop of carbon peaking and carbon neutrality, China's energy structure is undergoing a significant transformation (Zhang et al., 2023; Hou et al., 2023). The ongoing energy transition has triggered a measurable decline in traditional fossil fuel consumption, particularly for the refined oil (Qiu et al.,

* Corresponding author.
E-mail address: qliao@cup.edu.cn (Q. Liao).
Peer review under the responsibility of China University of Petroleum (Beijing).

https://doi.org/10.1016/j.petsci.2026.05.036

2022). In contrast, the production and utilization of clean liquid fuels such as green ammonia and methanol have expanded rapidly (Liao et al., 2022). Pipelines are widely regarded as the most promising mode of liquid fuel transportation due to their energy efficiency and uninterrupted delivery capabilities (Thompson and Farid, 2023). China's 14th Five-Year Plan (2021–2025) also emphasizes the strategic role of interconnected pipeline networks in ensuring the flexible and stable energy supply during the transition period. This national policy vision recognizes pipelines not just as transportation channels but as vital systemic platforms that must evolve to accommodate emerging energy vectors (Sidki et al., 2025). However, current pipeline infrastructure was historically designed for the unidirectional, fixed-route transportation of petroleum resources, which proves incompatible with the multidirectional and decentralized distribution patterns demanded by emerging renewable energy carriers (Acosta-Amado, 2024). As China accelerates its energy transition, this structural incompatibility poses critical challenges for adapting existing pipeline networks to accommodate emerging energy carriers (Manafi and Sayan, 2025).

A representative case is southwestern multi-product pipeline network in China, as seen in Fig. 1. The northern pipeline operates near full capacity, frequently failing to meet the demands of downstream stations. In contrast, the southern pipelines have a low utilization rate, so the pipeline company has carried out a reverse-flow plan to reallocate the remaining capacity from south to north (Tu et al., 2023a). To adapt to the requirements of reverse transportation volume, the stations along the pipeline have replaced or updated the pumps and pipeline segments along the line (Raoni et al., 2017). Aiming at this issue, this paper presents a techno-economic evaluation framework for pipeline reverse-flow retrofitting. Economic feasibility necessitates a comprehensive evaluation of the trade-off between the costs incurred by the retrofitting and the benefits of reverse transportation of new fuels. Technical feasibility considers the capability of existing pipelines and stations to support reverse-flow, including the control of pressure, flowrate and the contamination between oil batches, which is essential for evaluating whether the pipeline is operated safely.

To address the above research gaps, this paper proposes an optimization method coupled with a mixed-integer linear programming (MILP) model for the reverse-flow retrofitting of multi-product pipelines. The method systematically evaluates the feasibility of reverse flow within existing networks and automatically identifies economically optimal retrofit schemes when capacity is insufficient. By overcoming the limitations of experience-based judgments and single-scheme comparisons, the proposed framework integrates technical and economic evaluations at the planning stage, identifies key bottlenecks, and delivers practical retrofit pathways with clear engineering guidance.

1.2. Related work

1.2.1. Petroleum pipeline design optimization

Pipeline design has focused on balancing cost and performance under technical constraints. Cafaro et al. (2022) advanced the field by proposing a general mathematical programming framework applicable toliquid, gas, and multiphase flow pipelines. Ramos Rosa et al. (2018) introduced an MILP-based optimization for subsea pipeline networks, approximating nonlinear pressure drops via piecewise linearization. Despite transforming a complex Mixed-Integer Nonlinear Programming (MINLP) into a solvable form, their approach relies on predefined routes and suffers from high computational costs. Wang et al. (2019a) formulated a two-stage stochastic MILP model for steep-slope terrains, optimizing station layout and pipe diameter to manage pressure at critical points. In a related study, Wang et al. (2019b) proposed a thermo-hydraulic coupling method for crude oil pipelines, improving safety and economy under complex conditions. From a sustainability perspective, Zhou et al. (2020a) integrated economic and environmental goals using an enhanced ε-constraint method, generating Pareto frontiers for multi-objective decision-making. However, their use of fixed emission factors may limit the accuracy of carbon assessments. Across these studies, diameter optimization consistently targets cost reduction, while pressure control remains a key operational constraint.

1.2.2. Petroleum pipeline operations controlling

Recent research on liquid pipeline operation optimization has focused on contamination management, pressure control, and algorithmic efficiency. For contamination control, MirHassani and Ghorbanalizadeh (2008) introduced a discrete-time model with contamination volume as a decision variable. Xu et al. (2021) and Liao et al. (2018) reduced interface mixing through flowrate constraints and preprocessing techniques, respectively. In pressure control, Herrán et al. (2010) developed a multi-objective model balancing pumping costs, start-stop operations, and contamination losses. Reliability considerations were addressed by Zhou et al. (2020b), who proposed failure-mode flowrate limits, though partial pump degradation remains unmodeled. Chen et al. (2017) introduced a pump stability model requiring more comprehensive hydraulic integration. Liao et al. (2019) enabled real-time scheduling by decoupling event sequences, relying heavily on historical data. Two-stage approaches have addressed uncertainty: Garcia-Verdier et al. (2024) and Zhou et al. (2019) developed stochastic models for blending and supply chains, though scalability remains challenging. Collectively, these studies underscore that contamination control, pressure regulation, and computational efficiency are critical to stable pipeline operation. Accordingly, reverse-flow designs must maintain these parameters within safe bounds to

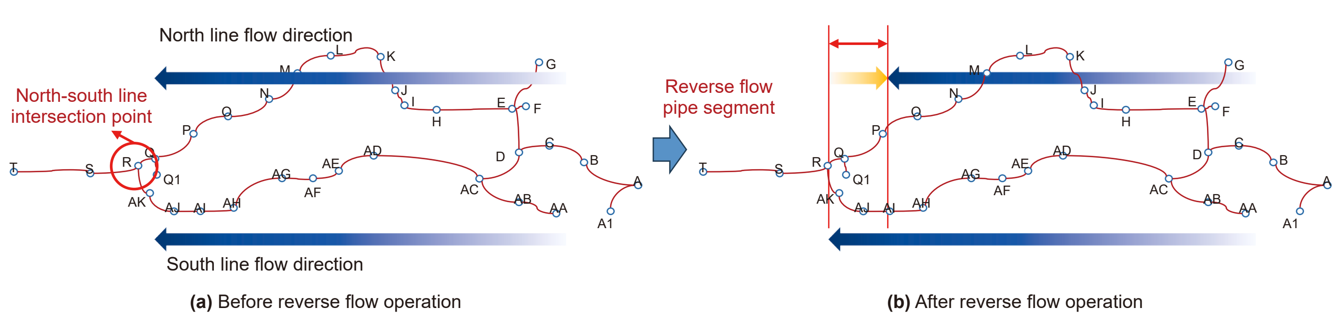

Fig. 1. Comparison of before and after reverse-flow of a multi-product pipeline network in China.

avoid excessive discharge pressure, insufficient intake pressure, or increased contamination.

1.2.3. Pipeline decommissioning and repurposing strategy

In the context of the energy transition, research has increasingly focused on the technical and economic feasibility of decommissioning and repurposing multi-product pipelines. For decommissioning, Li and Hu (2022, 2023) proposed a quasi-dynamic model integrating AHP and risk assessment to mitigate overfitting in traditional methods. Logsdon et al. (2025) developed a mixed-integer programming framework to optimize decommissioning strategies for small- and medium-scale networks. Regarding repurposing, Sandana et al. (2022) emphasized historical integrity data as a key criterion for identifying pipelines suitable for conversion. Spezakis and Xydis (2023) found that retrofitting existing pipelines for hydrogen transport can reduce costs by 35% compared to new cable systems. Further extending the scope, Liao et al. (2022, 2023) explored market-based allocation of residual pipeline capacity, while Li et al. (2022) proposed a balanced allocation method considering equity and efficiency. Tu et al. (2023b) found that biofuel transmission has limited impact on residual capacity allocation and later proposed a green ammonia supply chain framework using multi-product pipelines to reduce overall costs (Tu et al., 2024).

In summary, while existing research on unconventional transportation scenarios primarily remains at the planning stage, studies on critical pipeline parameters and contamination control focus on normal transportation conditions. This leaves a significant gap in reverse-flow optimization, hindering technical support for diverse transportation scenarios. Reverse-flow pipelines involve complex, high-order nonlinear constraints related to pressure and contamination, which often lead to excessive computation times and sub-optimal solutions for large-scale systems. Therefore, this work establishes an economic evaluation framework for multi-product pipeline reverse-flow, with the Module I focusing on the flowrate interval calculation, the Module II on the MILP model optimization and the Module III on the diameter correction. This framework enables both reverse-flow capacity calculation and renovating solution for multi-product pipelines.

1.3. Contributions of this work

Existing flow-direction optimization studies often oversimplify operational feasibility, creating disconnects between planning and implementation. The contributions of our work are listed as follows.

- A flowrate interval calculation method based on multi-modal control strategies is proposed to assess reverse-flow feasibility. If the flowrate interval is non-empty, it indicates that the existing engineering conditions support reverse-flow operation and flow regimes, pressure and product contamination are properly controlled.
- An integrated economic evaluation framework is developed to enhance reverse-flow capacity. By incorporating renovation measures, the model identifies cost-optimal retrofitting solutions and evaluates the financial performance of reverse-flow projects.
- Validation is conducted via a real-world case study of a major pipeline in China. Sensitivity analysis of key economic factors provides pipeline operators with actionable deployment-level and policy-oriented recommendations.

2. Problem description and solution approach

2.1. Problem description

This study first defines three fundamental metrics: transport capacity, actual flowrate, and pipeline utilization rate. Transport capacity is positively correlated with pipe diameter and refers to the maximum allowable oil volume per unit time for a given diameter. Actual flowrate is independent of diameter which refers to the actual volume of oil passing through the pipeline. Pipeline utilization rate refers to the ratio of actual flowrate to transport capacity. Higher utilization indicates better economic performance in pipeline design, while lower utilization implies wasted transport capacity and poorer economic performance.

The primary objective of employing variable pipe diameters in multi-product pipeline design is to reduce construction costs. Downstream flowrates decrease as product is delivered at distribution stations, maintaining a uniform diameter would result in excessive capacity and low utilization downstream. Consequently, downstream pipe segments are generally designed with smaller diameters (Fig. 2). To ensure operational feasibility, each segment is assigned a flowrate interval representing its permissible range of flowrates. In multi-product systems, delivery points cause these flowrates to fluctuate over time. The upper bound of this interval is determined by the minimum value derived from three multi-modal control strategies, including pressure control, flow-regime control, and multi-segment flowrate-coupling control strategy (Table 1). Conversely, the lower bound is the maximum value required by contamination control, flow regime control, and multi-segment flowrate-coupling control. It should be noted that the flow regime control and multi-segment flowrate-coupling control are applied simultaneously to the determination of both upper and lower bounds of flowrate intervals.

- Pressure control strategy: the upper bound is determined by the maximum allowable pressure drop (i.e., $\Delta p^{\max}$), which is a monotonically increasing function of the actual flowrate. The purpose of this strategy is to avoid over-pressure at the station outlet and under-pressure at the station inlet. Thus, the strategy is quantified as $\Delta p^{\max}$, defined as the difference between the maximum allowable pressure at the upstream station outlet and the minimum allowable pressure at the downstream station inlet).
- Flow regime control strategy: the upper bound is determined by the flow regime, which is classified according to the actual Reynolds number (i.e., Re, a monotonic function of the actual flowrate) and two critical Reynolds numbers (i.e., Re_1 and Re_2). The purpose of this strategy is to maintain the flow regime in either the hydraulically smooth or mixed-friction regime, both of which are typically observed in multi-product pipelines. Specifically, when $3000 < \mathrm{Re} < \mathrm{Re}_1$, the flow regime is hydraulically smooth; when $\mathrm{Re}_1 < \mathrm{Re} < \mathrm{Re}_2$, the flow regime is in the mixed-friction regime.
- Multi-segment flowrate-coupling control strategy: the upper bound is determined by the flowrates of adjacent segments. The flowrate intervals of different segments are mutually coupled. In a multi-source multi-sink pipeline, the upper bound of segment i cannot exceed the sum of downstream ($i1 > i$) flowrates or the sum of the upper bound of the segment $i-1$ and the injection station i.
- Contamination control strategy: the lower bound is determined by the development of contamination. The purpose of the strategy is to keep the development of interface mixing in a slow growth rate (i.e., $\mathrm{Re} > \mathrm{Re}_j$), where Re_j is a critical Reynolds number derived from contamination development behavior.

When flow direction is reversed, the original upstream pipeline becomes the downstream pipeline, which will result in the

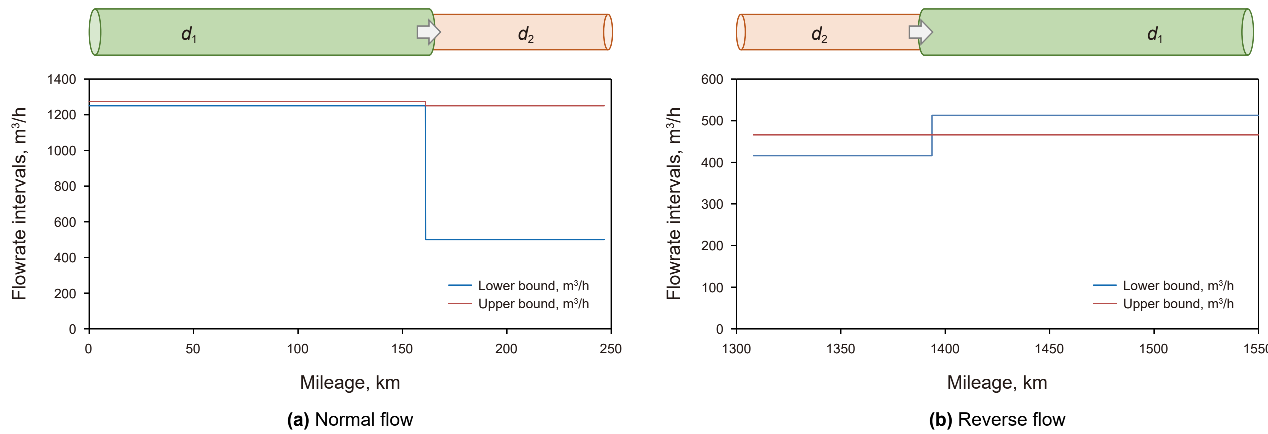

Fig. 2. Comparison of the flowrate intervals before and after reverse transportation flow direction.

Table 1
Description of multi-modal control strategies.

Control strategies	Related equations
Pressure control strategy	$\Delta p < \Delta p^{\max}$ $\Delta p = \rho^{\text{oil}} g \frac{\beta q^{2-\text{m}} \nu^{\text{m}}}{d^{5-\text{m}}} \cdot L$ $\Delta p^{\max} = p_i^{d,\max} - p_{i+1}^{s,\min}$
Flow regime control strategy	$3000 < \text{Re} < \text{Re}_1 = \frac{59.5}{\varepsilon^{8/7}}$ $\frac{59.5}{\varepsilon^{8/7}} = \text{Re}_1 < \text{Re} < \text{Re}_2 = \text{Re}_2 = \frac{665 - 765 \lg \varepsilon}{\varepsilon}$
Multi-segment flowrate coupling control strategy	Section 4.1
Contamination control strategy	$\frac{\nu d}{\upsilon} = \frac{4q}{\pi d \upsilon} = \text{Re} > \text{Re}_j = \text{Re}_j = 10000 \text{e}^{2.72 d^{0.5}}$

upstream pipe segment having a smaller diameter than the downstream pipe segment. The flowrate intervals may conflict with the original design. Under the pressure control strategy, the actual pressure loss (i.e., Δp) is a decreasing function of pipe diameter and an increasing function of flowrate. Given a fixed flowrate, a smaller diameter segment experiences a larger Δp. Once $\Delta p > \Delta p^{\max}$, the principle of "no over-pressure at the station outlet and under-pressure at the station inlet" is violated. Therefore, the flowrate must be reduced to enforce $\Delta p < \Delta p^{\max}$. The comparison of the flowrate intervals before and after reverse transportation (Fig. 2) shows that the flowrate interval of each segment declines to varying degrees. For large-diameter segments, if the flowrate interval were kept identical to that under normal transportation, severe interface contamination would occur. Moreover, considering the additional constraints from the flow regime control and the multi-segment flowrate coupling control strategy (i.e., MSFC), the original flowrate intervals are no longer valid. Hence, the flowrate intervals under the reverse-flow condition must be recalculated based on the multi-modal control strategies. Without retrofit of facilities, some large diameter downstream segments become infeasible for transportation. In principle, the upper bound of the flowrate interval should not be lower than the lower bound. Clearly, the flowrate interval of the green segments violates this rule (Fig. 2).

2.2. Solution approach

Reverse-flow operation is a design-centric task requiring comprehensive technical and economic assessments. Pipeline "transport capacity" is primarily dictated by design parameters, including pipe diameter, station and pipe design pressures, and segment flowrate intervals (Fig. 3). Since these parameters are typically optimized for normal flow, their suitability for reverse-flow conditions must be re-evaluated. This study recalculates permissible flowrate intervals under reverse-flow conditions while minimizing infrastructure changes by preserving existing design pressures and station flowrates. To prevent excessive pressure drops, severe interface mixing, or unstable flow regimes in pipeline segments, the flowrate interval is dynamically adjusted by incorporating multi-modal control strategies. The MILP model is developed to determine the transport capacity under the reverse-flow condition and to generate a technical-economically feasible operational plan. Subsequently, the study incorporates pipe segments renovations to further enhance the transport capacity, aiming to derive the most economically viable renovation solution. Here, the concept of "renovation" is reflected in the expansion of the flowrate interval and changes in pipe diameter. In other words, the MILP model introduces "pipe diameter" and "flowrate" as decision variables. However, the nonlinear relationship between pipe diameter and flowrate poses a challenge. To address this, piecewise linearization is applied to approximate the pipe diameter range. Initial application of this approximation may result in insufficient precision and incomplete satisfaction of process constraints. Therefore, the correction module is introduced to refine the pipe diameter, ensuring a more reasonable renovate solution that meets the technical feasibility requirements of both the transportation plan and the renovation plan under the reverse-flow condition. Finally, the feasibility of renovate project is evaluated by comparing the economic performance and transportation capacity before and after renovations.

3. Economic evaluation framework

The economic evaluation framework for reverse-flow project with renovation is shown in Fig. 4. Module I is used to calculate the

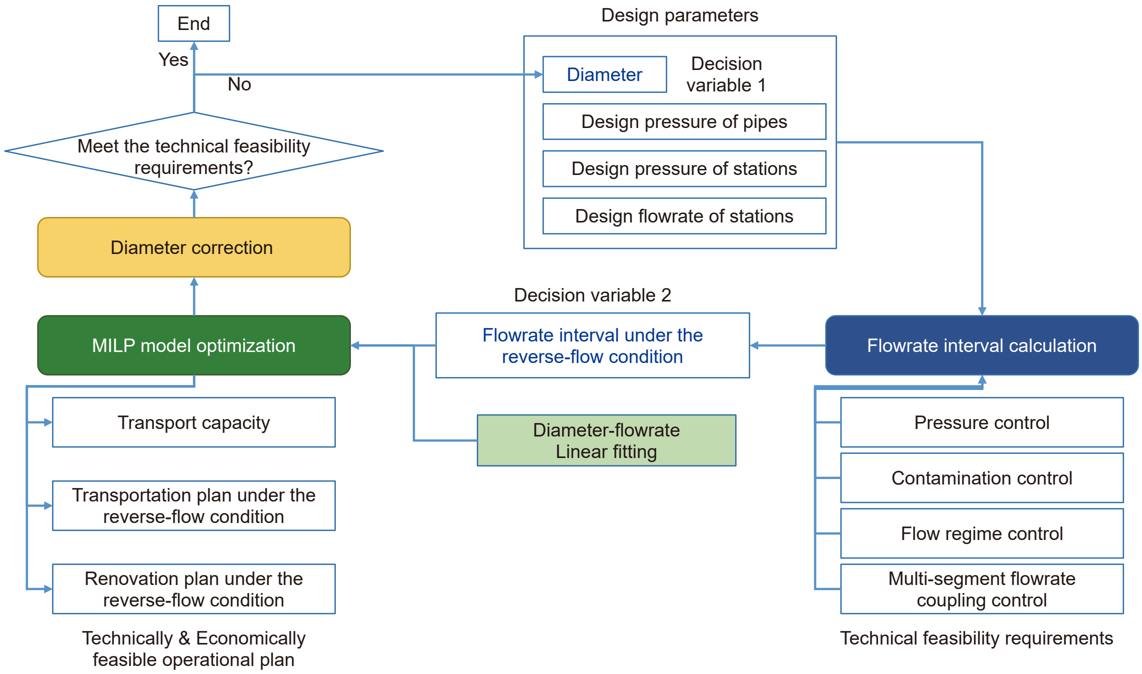

Fig. 3. Description of technical difficulties.

flowrate intervals, Module II is used to solve the MILP model for the retrofit scheme, and Module III is used to correct the pipe diameters and flowrate intervals. The workflow is as follows.

i) After initial parameter determination in Module I, the process proceeds to Module II for optimization.
ii) Once optimized, the results are fed back to Module I and checked against complex process requirements.
iii) If the process requirements are not satisfied, the correction module in Module III adjusts the pipe diameters until they comply with all constraints.
iv) Finally, a validated reverse-flow scheme with renovation that satisfies all process requirements.

3.1. Module I: Flowrate interval calculation

Module I of the economic evaluation framework calculates the flowrate interval for pipe segments, termed flowrate interval initialization (Fig. 5). This criterion determines the initial flowrate interval $\left[qp_i^{\min}, qp_i^{\max}\right]$ by integrating multi-modal control strategies, including contamination control strategy, pressure control strategy, flow regime control strategy and multi-segment flowrate coupling control strategy. i) The lower bound given by the contamination control strategy is denoted by qp_i^{mix}. ii) The upper bound given by the pressure control strategy is denoted by $qp_i^{\Delta p}$. iii) The upper bound given by the flow regime control strategy is denoted by qp_i^{lt}. iv) And the bounds derived from the multi-segment flowrate coupling strategy are expressed as $\min\left\{qd_{i1}^{\min} - qi_{i1}^{\max}, i1 \geq i+1\right\}$, $\sum_{i+1}^{\text{NI}} qd_{i1}^{\max} - qi_{i1}^{\min}$, $qp_{i-1}^{\max} + qi_i^{\max}$. Herein, the multi-segment flowrate coupling strategy combines three expressions related to the flowrates of adjacent segments or stations and yields both upper and lower bounds accordingly: $\min\left\{qd_{i1}^{\min} - qi_{i1}^{\max}, i1 \geq i+1\right\}$ contributes to the lower bound, while $\sum_{i+1}^{\text{NI}} qd_{i1}^{\max} - qi_{i1}^{\min}$ and $qp_{i-1}^{\max} + qi_i^{\max}$ contribute to the upper bound. Finally, the upper bound of the flowrate interval (i.e., $qp_i^{\max}$) is obtained as the minimum of $qp_i^{\Delta p}$, qp_i^{lt}, $qp_{i-1}^{\max} + qi_i^{\max}$, $\sum_{i+1}^{\text{NI}} qd_{i1}^{\max} - qi_{i1}^{\min}$, and the lower bound (i.e., $qp_i^{\min}$) is obtained as the maximum of qp_i^{mix}, $\min\left\{qd_{i1}^{\min} - qi_{i1}^{\max}, i1 \geq i+1\right\}$. Subsequently, the calculated initial flowrate intervals are substituted into Module II. The specific calculation equations can be found in Section 4.1.

3.2. Module II: MILP model optimization

Module II of the economic evaluation framework represents an MILP model, which is used to solve detailed reverse-flow schemes with renovation. The pipe segment flowrate boundaries $\text{QP}_i^{\min}/\text{QP}_i^{\max}$ are defined as continuous variables, and the initial flowrate intervals $qp_i^{\min}/qp_i^{\max}$ are taken as parameters for pipe segment flowrate constraints. When pipe segment flowrate boundaries $\text{QP}_i^{\min}/\text{QP}_i^{\max}$ deviate from the initial flowrate intervals $qp_i^{\min}/qp_i^{\max}$, it represents that the renovation behavior occurs. Considering general process constraints (e.g., time, oil volume, operation state, and operation volume constraints, as well as supply-demand balance) and special process constraints (e.g., operation flowrate, flowrate boundary, and pipe diameter constraints), the MILP model is established. The detailed formulation of the MILP model is presented in Section 4.2. With the objective of maximizing the difference between pipeline revenue and renovation cost, it is used to determine a reverse-flow scheme with renovated flowrate intervals and pipe diameters. In the conversion of flowrate intervals to pipe diameter, the least squares method is used to perform the piecewise linear fit of the flowrate-pipe

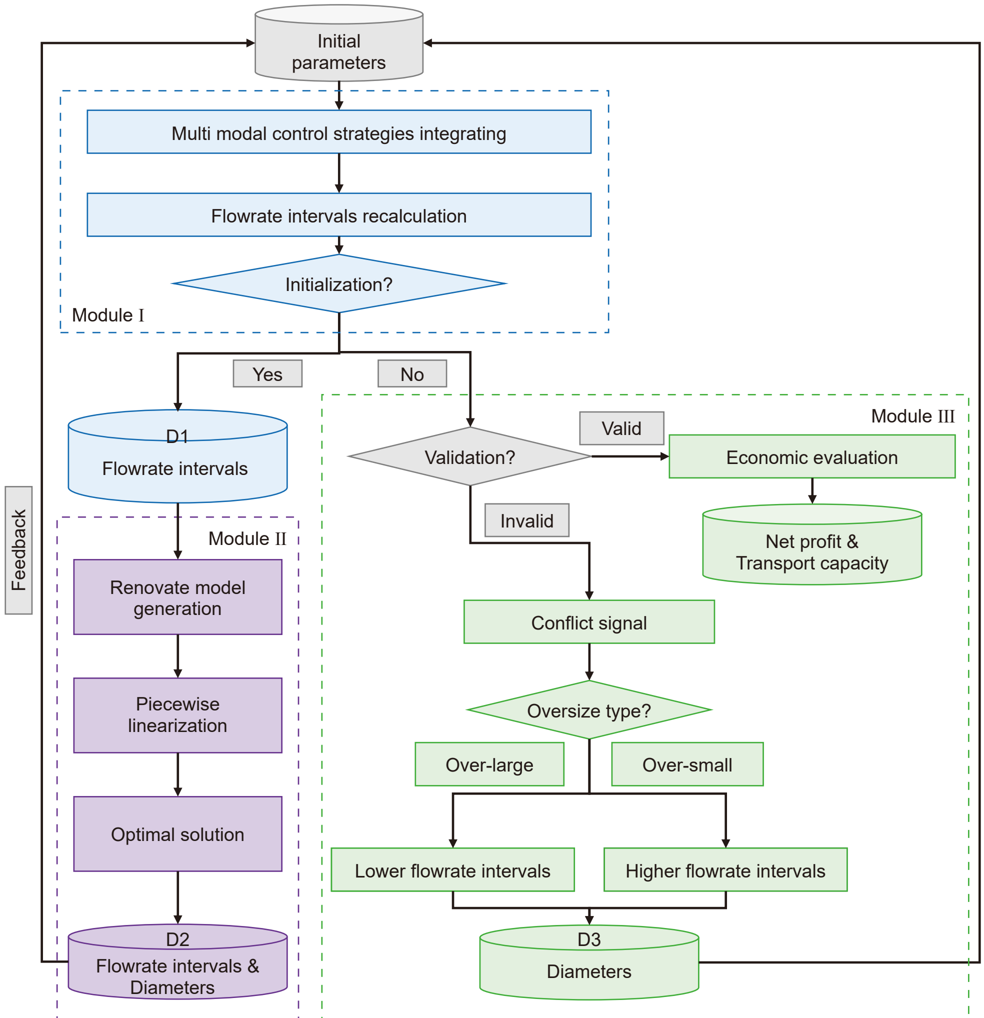

Fig. 4. Detailed data flow diagram of reverse-flow project with renovation.

diameter curve, thereby solving the nonlinear problem. After solving, the optimization results of pipe diameter and flowrate intervals are fed back to Module I of the economic evaluation framework through the feedback mechanism.

3.3. Module III: Diameter correction

After initial flowrate intervals $\left[qp_i^{\min}, qp_i^{\max}\right]$ are updated, if $\left[\mathrm{QP}_i^{\min},\ \mathrm{QP}_i^{\max}\right] \subseteq \left[qp_i^{\min},\ qp_i^{\max}\right]$, which represents higher-order nonlinear constraints have been satisfied, the calculation terminates. Otherwise, the calculation progress continues. Considering the low calculation accuracy of pipe segment diameter in Module II, Module III of the economic evaluation framework is used to correct diameter. Depending on the type of mutually exclusive progress constraints, either the diameter is adjusted downward or upward. After correction, the economic feasibility of reverse-flow project is evaluated using net benefit as the key indicator. The different scenarios of the correction module are described in Fig. 6. As shown in the figure, the optimization results and calculation results of the flowrate interval are the inputs of the correction module, which are classified into five scenarios according to their relative sizes, namely extremely pessimistic scenario (i.e., EPS), pessimistic scenario (i.e., PS), upper bound pessimistic scenario (i.e., UBPS), lower bound pessimistic scenario (i.e., LBPS) and optimistic scenario (i.e., OS). A description of five flowrate interval inputs is shown in Table 2. The ideal correction effect is that calculation results of flowrate intervals $\left[qp_i^{\min}, qp_i^{\max}\right]$ can completely cover optimization results $\left[\mathrm{QP}_i^{\min},\ \mathrm{QP}_i^{\max}\right]$, which is almost impossible to achieve. That is because during correction, the upper limit and lower limit of flowrate intervals $\left[qp_i^{\min}, qp_i^{\max}\right]$ are positively correlated with the pipe diameter. As the pipe diameter increases, the upper and lower limits of the flowrate interval rise simultaneously. Considering that the turnover is mainly determined by the upper limit, the upper limit $qp_i^{\max}$ is corrected accurately. Finally, the corrected upper limit $qp_i^{\max}$ is exactly the same as the optimization result $\mathrm{QP}_i^{\max}$. Unlike other scenarios, the upper limit $qp_i^{\max}$ is corrected downwards, as calculation results will likely align closer with optimization results in Lower Limit Pessimistic Scenario.

4. Methodology

4.1. Calculation criteria for pipe segment flowrate intervals

As described in Section 3, Module I of the economic evaluation framework is used to calculate the initial values of pipe segment

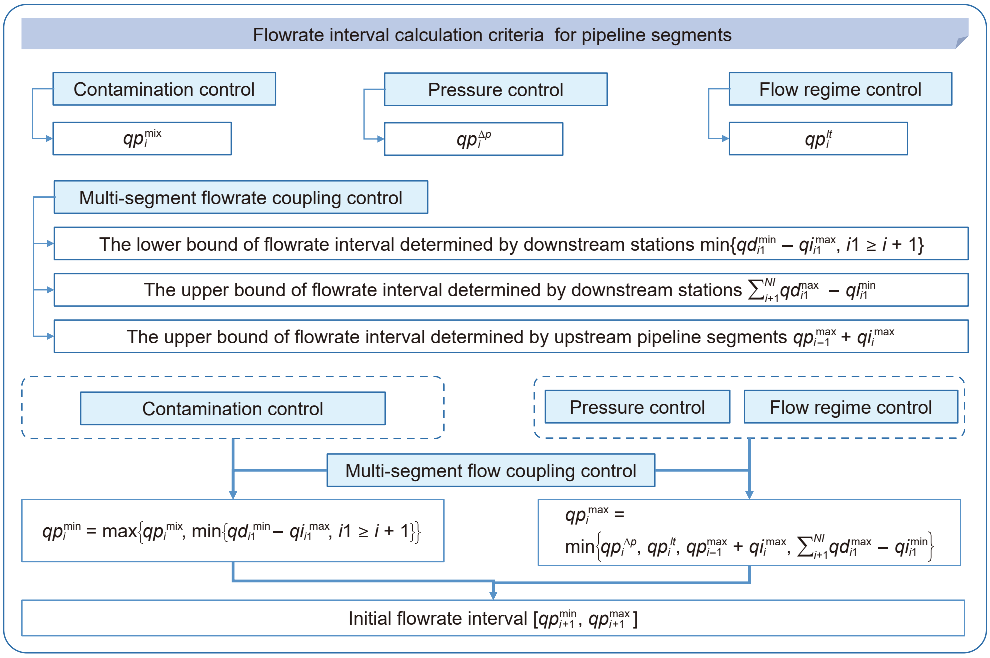

Fig. 5. The calculation criterion for flowrate intervals in Module I of the economic evaluation framework.

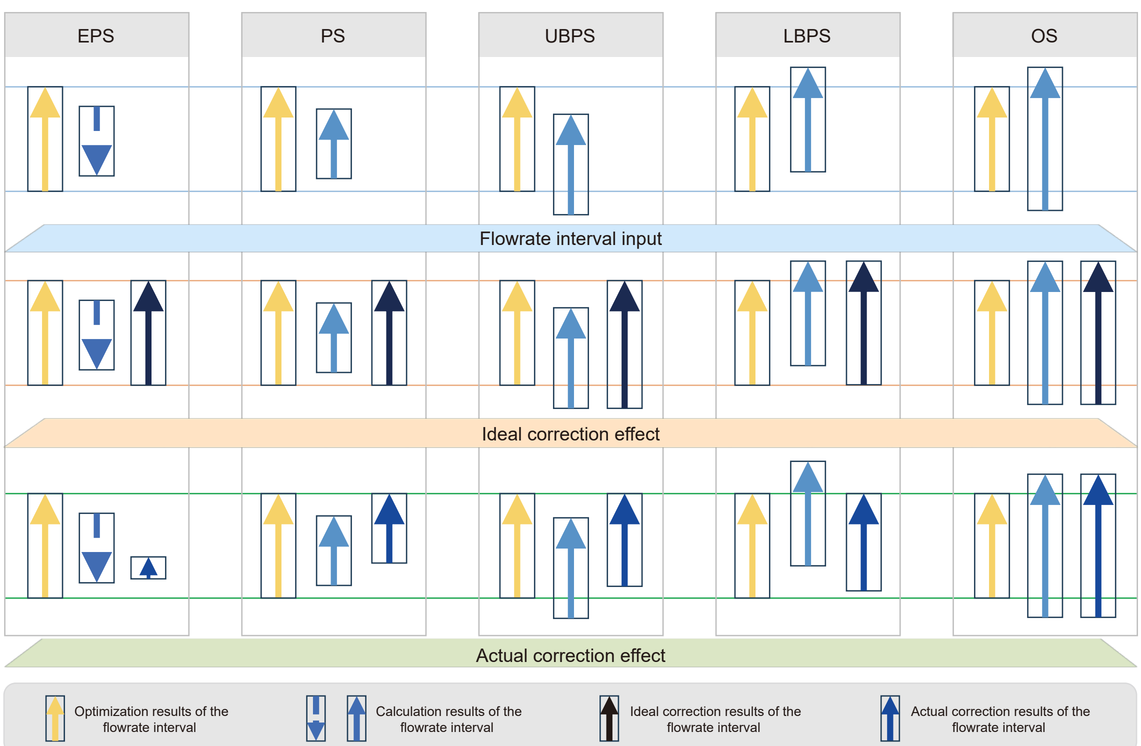

Fig. 6. Correction effect of different scenarios in the correction module.

flowrate intervals that satisfy the higher-order nonlinear constraints, combining mixing control conditions, pressure control conditions and flow regime control conditions, and flowrate equilibrium relationships between pipe segments. This section expands on the calculation criteria, as shown in Eqs. (1)–(5).

(1) Lower bound defined by contamination control strategy

Once the flow direction in a pipe segment is altered, the development of contamination must be kept under stable control. In other words, the Reynolds number must be greater than the

Table 2
Description of flowrate interval inputs.

Flowrate interval input scenario	Description	Related equations
Extremely pessimistic scenario	The calculation results of flowrate intervals $\left[qp_i^{\min}, qp_i^{\max}\right]$ do not correspond to the regular physical laws.	$\left[qp_i^{\min}, qp_i^{\max}\right] = \varnothing$
Pessimistic scenario	The calculation results of flowrate intervals $\left[qp_i^{\min}, qp_i^{\max}\right]$ do not cover the optimization results of flowrate intervals $\left[\mathrm{QP}_i^{\min}, \mathrm{QP}_i^{\max}\right]$.	$\left[\mathrm{QP}_i^{\min}, \mathrm{QP}_i^{\max}\right] \cap \left[qp_i^{\min}, qp_i^{\max}\right] = \left[qp_i^{\min}, qp_i^{\max}\right]$
Upper limit pessimistic scenario	The upper limit $qp_i^{\max}$ of the calculation results does not cover the optimization results $\mathrm{QP}_i^{\max}$ of flowrate intervals.	$\left[\mathrm{QP}_i^{\min}, \mathrm{QP}_i^{\max}\right] \cap \left[qp_i^{\min}, qp_i^{\max}\right] = \left[\mathrm{QP}_i^{\min}, qp_i^{\max}\right]$
Lower limit pessimistic scenario	The lower limit $qp_i^{\min}$ of the calculation results does not cover the optimization result $\mathrm{QP}_i^{\min}$ of flowrate intervals.	$\left[\mathrm{QP}_i^{\min}, \mathrm{QP}_i^{\max}\right] \cap \left[qp_i^{\min}, qp_i^{\max}\right] = \left[qp_i^{\min}, \mathrm{QP}_i^{\max}\right]$
Optimistic scenario	The calculation results of flowrate intervals $\left[qp_i^{\min}, qp_i^{\max}\right]$ can fully cover the optimization results of flowrate intervals $\left[\mathrm{QP}_i^{\min}, \mathrm{QP}_i^{\max}\right]$.	$\left[\mathrm{QP}_i^{\min}, \mathrm{QP}_i^{\max}\right] \cap \left[qp_i^{\min}, qp_i^{\max}\right] = \left[\mathrm{QP}_i^{\min}, \mathrm{QP}_i^{\max}\right]$

critical Reynolds number (Eq. (1)). The corresponding lower bound is derived as expressed in Eqs. (1) and (2):

$$\frac{4qp_i^{\text{mix}}}{\pi d \nu} \geq 10000\mathrm{e}^{2.72d^{0.5}} \tag{1}$$

$$qp_i^{\text{mix,min}} = \frac{10^4 \pi d \nu \mathrm{e}^{2.72d^{0.5}}}{4}, \forall i < |\mathrm{I}| \tag{2}$$

where d represents inner diameter of pipe segments, m; ν represents the viscosity of oil, m^2/s; $qp_i^{\text{mix,min}}$ represents the lower bound defined by oil mixing control conditions, m^3/s.

(2) Upper bound defined by pressure control strategy

Once the flow direction of the pipe segments are reversed, the actual pressure drop along the pipeline must not exceed the theoretical maximum, as shown in Eq. (3). The corresponding upper bound is derived in Eq. (4).

$$\rho^{\text{oil}} g \frac{\beta \nu^m dl \left(qp_i^{\Delta p}\right)^{2-m}}{d^{5-m}} \leq \Delta p^{\max} \tag{3}$$

$$qp_i^{\Delta \mathrm{p,max}} = \left(\frac{\Delta p^{\max} d^{5-m}}{\rho^{\text{oil}} g \beta \nu^m \cdot dl}\right)^{\frac{1}{2-m}}, \forall i < |\mathrm{I}| \tag{4}$$

Here ρ^{oil} represents oil density, $\mathrm{kg/m}^3$; g represents the gravitational acceleration, $\mathrm{m/s}^2$; dl represents pipe segments length, m; $qp_i^{\Delta \mathrm{p,max}}$ represents the upper bound defined by pressure control conditions, m^3/s.

(3) Upper bound defined by flow regime control strategy

Once the flow direction of the pipe segments is reversed, the oil flow regime must be maintained within the hydraulically smooth zone, as expressed in Eq. (5). Consequently, the upper bound is derived in Eq. (6).

$$\frac{4qp_i^{lt}}{\pi d \nu} \leq \frac{59.5}{\varepsilon^{\frac{8}{7}}} \tag{5}$$

$$qp_i^{lt,\max} = \frac{59.5 \pi d \nu}{4 \varepsilon^{\frac{8}{7}}}, \forall i < |\mathrm{I}| \tag{6}$$

Here ε represents the relative roughness; $qp_i^{lt,\max}$ represents the upper bound defined by flow regime control conditions, m^3/s.

(4) Lower bound and upper bound defined by multi-segment flowrate coupling control strategy

The lower bound of pipe segments is related to the lower bound of the downstream stations, as shown in Eq. (7). The upper bound depends not only on upper bound of the upstream pipe segment and the injection station, but also on the sum of operation bounds of the downstream stations, as shown in Eq. (8).

$$qp_i^{\text{mul-seg,min}} = \min_{i1 \geq i+1} qd_{i1}^{\min} - qi_{i1}^{\max}, \forall i < |\mathrm{I}| \tag{7}$$

$$qp_i^{\text{mul-seg,max}} = \min\left\{qp_{i-1}^{\max} + qi_i^{\max}, \sum_{i+1}^{\mathrm{NI}} qd_{i1}^{\max} - qi_{i1}^{\min}\right\}, \forall 1 < i < |\mathrm{I}| \tag{8}$$

Here $qp_i^{\text{mul-seg,min}}$ represents the lower bound defined by the lower bound of the downstream stations, m^3/s; $qp_{i-1}^{\max}$ represents the upper bound of the upstream pipe segment, m^3/s; $\sum_{i+1}^{\mathrm{NI}} qd_{i1}^{\max}$ represents the sum of bounds of the downstream stations, m^3/s; $qi_{i1}^{\max}/qi_{i1}^{\min}$ represents the upper bound and the lower bound of the upstream injection station, respectively, m^3/s.

(5) Ultimate value of pipe segment flowrate interval

The lower bound of a pipe segment is the maximum value between the contamination-defined lower bound and the MSFC-defined lower bound (Eq. (9)), and the upper bound is the minimum value among the pressure-defined upper bound, the flow regime-defined upper bound, and the MSFC-defined upper bound (Eq. (10)).

$$qp_i^{\min} = \max\left\{qp_i^{\text{mix,min}}, qp_i^{\text{mul-seg,min}}\right\}, \forall i < |\mathrm{I}| \tag{9}$$

$$qp_i^{\max} = \min\left\{qp_i^{\Delta \mathrm{p,max}}, qp_i^{\mathrm{lt,max}}, qp_i^{\text{mul-seg,max}}\right\}, \forall i < |\mathrm{I}| \tag{10}$$

Here $qp_i^{\max}/qp_i^{\min}$ represents ultimate value of pipe segment flowrate interval, m^3/h.

4.2. Mathematical model

This section elaborates on Module II of the economic evaluation framework. The model takes maximizing the net benefit of reverse-flow as its objective, which introduces general process constraints and the special process constraints such as operational flowrate constraints, flowrate interval constraints, and pipe diameter constraints. Finally, the transformation scheme is decided including the pipe diameters and the flowrate intervals.

4.2.1. Objective function

The pipeline's net benefit is defined as the total revenue f_1 minus operating cost f_2. The renovation cost consists of two parts: material cost f_3 and construction cost f_4. The construction cost f_4 consists of the emptying cost, excavation cost, old pipe treatment cost and new pipe backfill cost. The objective function is given by Eqs. (11)–(15):

$$\max f = f_1 - f_2 - \chi(f_3 + f_4) \tag{11}$$

$$f_1 = \sum_{t\in|\mathrm{T}|}\sum_{i\in \mathrm{I}^{\mathrm{d}}} \varepsilon_1 \rho^{\mathrm{oil}} c^{\mathrm{tran}} \mathrm{VD}_{t,i} L_i \tag{12}$$

$$f_2 = \sum_{t\in|\mathrm{T}|}\sum_{i\in \mathrm{I}^{\mathrm{d}}} \varepsilon_1 \rho^{\mathrm{oil}} c^{\mathrm{run}} \mathrm{VD}_{t,i} L_i \tag{13}$$

$$f_3 = \sum_{i\in|\mathrm{I}|} \varepsilon_2 c^{\mathrm{pur}} \rho^{\mathrm{steel}} \pi \mathrm{RM}_i \delta_i \cdot dl_i \tag{14}$$

$$f_4 = \sum_{i\in|\mathrm{I}|}\left(c^{\mathrm{lay}} + c_i^{\mathrm{empty}} + c^{\mathrm{exa}} + c^{\mathrm{deal}}\right)\mathrm{RM}_i \cdot dl_i \tag{15}$$

where RM_i is an auxiliary variable, when pipe segment is not renovated, $\mathrm{RM}_i = 0$, otherwise, $\mathrm{RM}_i = \mathrm{DS}_i$; $\varepsilon_1/\varepsilon_2$ represent unit conversion coefficients, whose values are respectively 1×10^{-3} and 1×10^{-6}; χ represents the coefficient used to convert the payback period pb to the planning cycle tl, $\chi = \frac{tl}{350\times 24\times pb}$; $\rho^{\mathrm{oil}}/\rho^{\mathrm{steel}}$ respectively represents oil density and steel density, kg/ m^3; c^{tran} represents pipeline unit transport revenue, CNY/(t·km); c^{run} represents unit operating cost, CNY/(t·km); c^{pur} represents acquisition unit cost, CNY/t; c^{lay} represents backfill unit cost, CNY/(mm·km); c_i^{empty} represents emptying cost, CNY/km; c^{exa} represents excavation cost, CNY/km; c_i^{deal} represents pipe treatment cost, CNY/ km; $\mathrm{VD}_{t,i}$ represents the actual delivery volume from station i during slot t, m^3; L_i represents the mileage from the initial station to station i, km; dl_i represents the length of pipe segment i, km.

4.2.2. General constraints

(1) Pipe segment operation status

The optimization model requires identifying the operational status of pipe segments, which are categorized into operating and shutdown states. These states are represented by binary variable $\mathrm{BP}_{t,i}$, where $\mathrm{BP}_{t,i} = 1$ indicates that pipe segment i is in the operating state at time t and $\mathrm{BP}_{t,i} = 0$ signifies a shutdown. For the delivery station i, when an upstream pipe segment i is shutdown, the downstream pipe segment $i+1$ must be shutdown (see Eq. (16)). For the injection station i, when a downstream pipe segment $i+1$ is shutdown, the upstream pipe segment i must be shutdown (see Eq. (17)).

$$\mathrm{BP}_{t,i+1} \le \mathrm{BP}_{t,i}\ \forall t\in|\mathrm{T}|, i\in \mathrm{I}^{\mathrm{d}} \tag{16}$$

$$\mathrm{BP}_{t,i+1} \ge \mathrm{BP}_{t,i}\ \forall t\in|\mathrm{T}|, i\in \mathrm{I}^{\mathrm{i}} \tag{17}$$

(2) Pipe segment flowrate constraints

The pipeline system consists of stations and pipe segments, in which the stations are divided into injection stations and delivery stations based on their functional attributes. When pipe segment i is active, its upstream flowrate is greater than the difference between the downstream station's delivery flowrate and injection flowrate, as shown in Eq. (18). Conversely, if the segment is idle, the flowrate is forced to zero as shown in Eq. (19).

$$\frac{\sum\limits_{i'\ge i+1}\mathrm{VD}_{t,i'} - \sum\limits_{i'\ge i+1}\mathrm{VI}_{t,i'}}{dt} \le \mathrm{QP}_i^{\max} + \left(1-\mathrm{BP}_{t,i}\right)\frac{vc}{dt}, \forall t\in|\mathrm{T}|, i\in|\mathrm{I}| \tag{18}$$

$$\frac{\sum\limits_{i'\ge i+1}\mathrm{VD}_{t,i'} - \sum\limits_{i'\ge i+1}\mathrm{VI}_{t,i'}}{dt} \le \mathrm{BP}_{t,i}\frac{vc}{dt}, \forall t\in|\mathrm{T}|, i\in|\mathrm{I}| \tag{19}$$

where $\mathrm{VD}_{t,i'}$ represents the delivery volume of station i' during slot t, m^3; $\mathrm{VI}_{t,i'}$ represents the injection volume of station i' during slot t, m^3; $\mathrm{QP}_i^{\max}$ represents the upper bound of pipe segment flowrate, m^3/h; dt represents the time interval t, with the value of 24 h.

In any time slot, the operation volume of the first pipe segment $\mathrm{VP}_{t,\,i=1}$ is the same as the injection volume of the initial station $\mathrm{VI}_{t,\,i=1}$, as shown in Eq. (20). The operation volume in the downstream pipe segment $i+1$ is equal to the operation volume in the upstream pipe segment i minus the delivery volume of the upstream station $i+1$, plus the injection volume of the upstream station $i+1$, as shown in Eq. (21). Eq. (22) is used to constrain the coupling relationship between the operation volume, the delivery volume and the injection volume during slot t.

$$\mathrm{VP}_{t,i=1} = \mathrm{VI}_{t,i=1}, \forall t\in|\mathrm{T}| \tag{20}$$

$$\mathrm{VP}_{t,i+1} = \mathrm{VP}_{t,i} - \mathrm{VD}_{t,i+1} + \mathrm{VI}_{t,i+1}, \forall t\in|\mathrm{T}|, i<|\mathrm{I}| \tag{21}$$

$$\sum_{t\in|\mathrm{T}|}\mathrm{VP}_{t,i+1} + \sum_{t\in|\mathrm{T}|}\mathrm{VD}_{t,i+1} - \sum_{t\in|\mathrm{T}|}\mathrm{VI}_{t,i+1} \le \sum_{t\in|\mathrm{T}|}\mathrm{VP}_{t,i} + \mathrm{VB}_{t=1}, \forall i<|\mathrm{I}| \tag{22}$$

where $\mathrm{VP}_{t,i}$ represents the operation volume of pipe segment i during slot t, m^3, and $\mathrm{VB}_{t=1}$ represents the oil volume in pipeline at the initial moment, m^3.

(3) Supply and demand balance constraints

For a pipeline system, the total supply from injection stations is equal to the total demand from delivery stations at any time interval. Supply and demand equilibrium constraint is expressed in Eq. (23).

$$\sum_{i\in \mathrm{I}^{\mathrm{i}}}\mathrm{VI}_{t,i} = \sum_{i\in \mathrm{I}^{\mathrm{d}}}\mathrm{VD}_{t,i}, \forall t\in|T| \tag{23}$$

4.2.3. Special constraints

Pipe segments require renovation to increase capacity prior to reverse-flow operations. To model this, we define the binary decision variable XE_i indicating whether segment i undergoes renovation. The renovation project incorporates process-specific constraints including flowrate limitations, renovation decisions, and pipe diameter requirements. Continuous variable $\mathrm{QP}_i^{\max}$/$\mathrm{QP}_i^{\min}$ is respectively defined as the upper and lower bound of the pipe segment flowrate after renovation. Continuous variable $\mathrm{QI}_i^{\max}$/$\mathrm{QI}_i^{\min}$ is respectively defined as injection upper and lower bound after renovation. Continuous variable DS_i is defined as diameter of pipe segment i after renovation.

(1) Operation flowrate constraints

Only when the upper and lower bound of the operation flowrate requirements are met, will it be allowed to perform. Otherwise, the operation request will be rejected.

The initial station adopts continuous injection mode, whose injection flowrate constraints are shown in Eq. (24). The intermediate injection stations adopt concentrated injection mode, whose injection flowrate constraints are shown in Eq. (25). Eq. (26) is used to describe the non-injection status.

$$\mathrm{QI}_{i=1}^{\min}dt-(1-\mathrm{BI}_{t,i})vc\le \mathrm{VI}_{t,i}\le \mathrm{QI}_{i=1}^{\max}dt+(1-\mathrm{BI}_{t,i})vc,\forall t\in|\mathrm{T}|,i=1 \tag{24}$$

$$\mathrm{VI}_{t,i}\le \mathrm{QI}_i^{\max}dt+(1-\mathrm{BI}_{t,i})vc,\forall t\in|\mathrm{T}|,i\in \mathrm{I}^{\mathrm{i}}\backslash \mathrm{I}^{\mathrm{f}} \tag{25}$$

$$\mathrm{BI}_{t,i}m\le \mathrm{VI}_t\le \mathrm{BI}_{t,i}vc,\forall t\in|\mathrm{T}|,i\in \mathrm{I}^{\mathrm{i}} \tag{26}$$

Here $\mathrm{BI}_{t,i}$ is binary variable that indicates the operational status of injection station i during slot t; $\mathrm{QI}_i^{\max}$/$\mathrm{QI}_i^{\min}$ respectively represents the flowrate upper and lower bound of the injection station i, m^3/ h.

Delivery stations employ a centralized delivery process where delivery volumes are smaller than in continuous delivering. The discrete time slots under centralized delivering cannot align with those under continuous delivering. Consequently, no lower bound constraint is imposed on delivery flowrate. Specific constraints are detailed in Eqs. (27) and (28). Similarly, pipe segment flowrate constraints are shown in Eqs. (29) and (30).

$$\mathrm{VD}_{t,i}\le \mathrm{BD}_{t,i}qd_i^{\max}dt,\forall t\in|\mathrm{T}|,i\in \mathrm{I}^{\mathrm{d}} \tag{27}$$

$$\mathrm{VD}_{t,i}\le qd_i^{\max}dt,\forall t\in|\mathrm{T}|,i\in \mathrm{I}^{\mathrm{d}} \tag{28}$$

$$\begin{aligned}&\mathrm{QP}_i^{\min}dt-(1-\mathrm{BP}_{t,i})vc\le \mathrm{VP}_{t,i}\le \mathrm{QP}_i^{\max}dt\\&+(1-\mathrm{BP}_{t,i})vc,\forall t\in|\mathrm{T}|,i\in|\mathrm{I}|\end{aligned} \tag{29}$$

$$\mathrm{BP}_{t,i}m\le \mathrm{VP}_{t,i}\le \mathrm{BP}_{t,i}vc,\forall t\in|\mathrm{T}|,i\in|\mathrm{I}| \tag{30}$$

Here $\mathrm{BD}_{t,i}$ is binary variable that indicates the operational status of delivery station i during slot t; $qd_i^{\max}$/$qd_i^{\min}$ represent the upper and lower bound of the station i flowrate, m^3/h; $\mathrm{QP}_i^{\max}$/$\mathrm{QP}_i^{\min}$ represents the upper and lower bounds of pipe segment i flowrate, m^3/h; $\mathrm{VP}_{t,i}$ represents the operation volume of pipe segment i during slot t, m^3.

(2) Decisions on whether to renovate pipe segments

Binary variable XE_i is defined as whether pipe segment i is renovated or not. Continuous variables $\mathrm{QI}_i^{\max}$/$\mathrm{QI}_i^{\min}$/$\mathrm{QP}_i^{\max}$/$\mathrm{QP}_i^{\min}$ are defined as flowrate bounds after renovation. If the above continuous variables deviate from parameters $qi_i^{\max}$/$qi_i^{\min}$/$qp_i^{\max}$/$qp_i^{\min}$, renovation will be triggered and $\mathrm{XE}_i=1$. The judgement expressions of renovation are shown in Eqs. (31)–(34):

$$(\mathrm{XE}_i m+1)qp_i^{\max}\le \mathrm{QP}_i^{\max}\le(\mathrm{XE}_i fac+1)qp_i^{\max},\forall i\in|\mathrm{I}| \tag{31}$$

$$(1-\mathrm{XE}_i fac)qp_i^{\min}\le \mathrm{QP}_i^{\min}\le(1-\mathrm{XE}_i m)qp_i^{\min},\forall i\in|\mathrm{I}| \tag{32}$$

$$(\mathrm{XE}_i m+1)qi_i^{\max}\le \mathrm{QI}_i^{\max}\le(\mathrm{XE}_i fac+1)qi_i^{\max},\ i=1 \tag{33}$$

$$(1-\mathrm{XE}_i fac)qi_i^{\min}\le \mathrm{QI}_i^{\min}\le(1-\mathrm{XE}_i m)qi_i^{\min},\ i=1 \tag{34}$$

where m represents minimum; fac represents flowrate interval expansion factor.

(3) Pipe diameter constraints

Continuous variable DS_i represents the standard pipe diameter after renovation, while binary variable $\mathrm{STA}_{i,n}$ indicates whether the diameter of pipe segment i is equal to standard diameter n. Logic constraints are established among $\mathrm{STA}_{i,n}$, XE_i, and $\mathrm{QP}_i^{\max}$. Although the theoretical relationship between DS_i and $\mathrm{QP}_i^{\max}$ is nonlinear as shown in Eq. (35), a linear approximation is derived using the least squares method to determine the slope a_i and intercept b_i. In Eqs. (36) and (37). However, DS_i cannot be directly substituted into the objective function because renovation costs (f_3+f_4) must be zero if no renovation occurs. Therefore, auxiliary variable RM_i is introduced. This variable ensures that RM_i is equal to DS_i when renovation occurs, whereas both RM_i and the associated renovation costs are equal to zero, see Eq. (38). The large constant M in Eqs. (36)–(38) represents the maximum value.

Table 3
General parameters.

Parameters	Value (Reasonable range)	Parameters	Value (Reasonable range)
a_i/ b_i, mm/ (m^3 /h)/ 1	0.3409/173	c^{exa}, CNY/km	430
c^{tran}, CNY/ (t·km)	0.196 (0.146–0.246)	fac	0.18 (0.02–0.18)
c^{run}, CNY/ (t·km)	0.1	pb, a	8 (5–9)
c^{pur}, CNY/ t	6000 (4000–8000)	ρ^{oil}, $\mathrm{kg/m^3}$	750/850/800
c^{lay}, CNY/ (mm·km)	500	ρ^{steel}, $\mathrm{kg/m^3}$	7850
c_i^{empty}, CNY/ km	162	tl, h	360
c_i^{deal}, CNY/ km	121	v, m/s	1.5 (1–2)

$$\mathrm{DS}_i = \sqrt{\frac{4\mathrm{QP}_i^{\max}}{\pi v}} \tag{35}$$

$$a_i\mathrm{QP}_i^{\max} + b_i - (1-\mathrm{XE}_i)M \le \mathrm{DS}_i \le a_i\mathrm{QP}_i^{\max} + b_i + (1-\mathrm{XE}_i)M, \forall i \in |\mathrm{I}| \tag{36}$$

$$-\mathrm{XE}_i\mathrm{M} + d_i \le \mathrm{DS}_i \le \mathrm{XE}_iM + d_i, \forall i \in |\mathrm{I}| \tag{37}$$

$$\mathrm{RM}_i \ge \mathrm{DS}_i - (1-\mathrm{XE}_i)M, \forall i \in |\mathrm{I}| \tag{38}$$

Since the pipeline renovation project is essentially a construction project, the diameter needs to meet the national standards in construction process. In the model, the continuous variable diameter DS_i is transformed into the discrete variable. Meanwhile, binary variable $\mathrm{STA}_{i,n}$ and standard diameter library d_n^{lib} are introduced to align diameter DS_i with standard diameter d_n^{lib}. Detailed constraints are shown in Eqs. (39) and (40). Besides, additional constraints are introduced to reflect the association between binary variable $\mathrm{STA}_{i,n}$ and binary variable XE_i, as shown in Eq. (40).

$$d_n^{\mathrm{lib}} - (1-\mathrm{STA}_{i,n})\mathrm{M} \le \mathrm{DS}_i \le d_n^{\mathrm{lib}} + (1-\mathrm{STA}_{i,n})\mathrm{M}, \forall i \in |\mathrm{I}|, n \in \mathrm{N} \tag{39}$$

$$\sum\nolimits_{n\in\mathrm{N}} \mathrm{STA}_{i,n} = \mathrm{XE}_i, \forall i \in |\mathrm{I}| \tag{40}$$

4.3. Linear fitting of diameter-flowrate

Section 3.3 points out that standard diameter DS_i is derived from $\mathrm{QP}_i^{\max}$, which exhibits a non-linear relationship (Eq. (41)). In this section, the least squares method is adopted for linearization. First, the variable $\mathrm{QP}_i^{\max}$ is divided into several small intervals $\left[qp_i^{\max},\right.$

Table 4
Pipe parameters.

Station number	$qd_i^{\max}$, m^3/h	$qd_i^{\min}$, m^3/h	L_i, km	D_i^{out}, mm	δ_i, mm	$dp^{\max}$, MPa
1	0	0	0	273.1	5.6	9.5
2	280	100	60.4	406.4	6.4	8.8
3	480	40	205	406.4	7.1	9.5
4	80	25	292.97	406.4	7.1	9.5
5	80	25	371.57	406.4	7.4	8.8
6	280	40	484.81	406.4	7.1	9.5
7	500	40	581.19	457	7.9	9.5
8	150	40	680.09	457	7.1	8.7
9	150	40	939.27	457	7.1	8.7
10	500	180	1097.27	508	7.1	7
11	600	50	1244.56	457	7.1	8.7
12	200	40	1308.15	457	7.1	8.7
13	200	40	1393.68	508	7.1	7
14	513	464	1554.77	–	–	–

Table 5
Calculation of the initial values of flowrate intervals for reverse-flow process.

Pipe segment number	$qp_i^{\min}$, m^3/h	$qp_i^{\max}$, m^3/h	Sub item $qp_i^{\min}$, m^3/h		Sub item $qp_i^{\max}$, m^3/h		
			Contamination control	MSFC control 1	Pressure & flow regime control	MSFC control 2	MSFC control 3
1	162	466	162	25	466	–	4013
2	333	466	333	25	814	466	3733
3	331	466	331	25	1120	466	3253
4	331	466	331	25	1191	466	3173
5	330	466	330	40	926	466	3093
6	331	466	331	40	1066	466	2813
7	413	466	413	40	1441	466	2313
8	416	466	416	40	799	466	2163
9	416	466	416	40	1060	466	2013
10	513	466	513	40	1311	466	1513
11	416	466	416	40	1776	466	913
12	416	466	416	40	1500	466	713
13	513	466	513	464	1245	466	513

Table 6
Economic results and total renovated capacity for non-standardized diameters scenario.

Stage	Net benefit, 10^4CNY	Transportation revenue, 10^4CNY	Renovation cost, 10^4CNY	Turnover, 10^8t·km	Renovated pipe capacity, $10^4 m^3$
Pre-renovation	1348.8	1348.8	0	1.4050	0
Pre-correction	1372.8	1497.0	123.9	1.559	3.2374
Post-correction	1668.9	1878.0	209.0	1.9562	3.1483

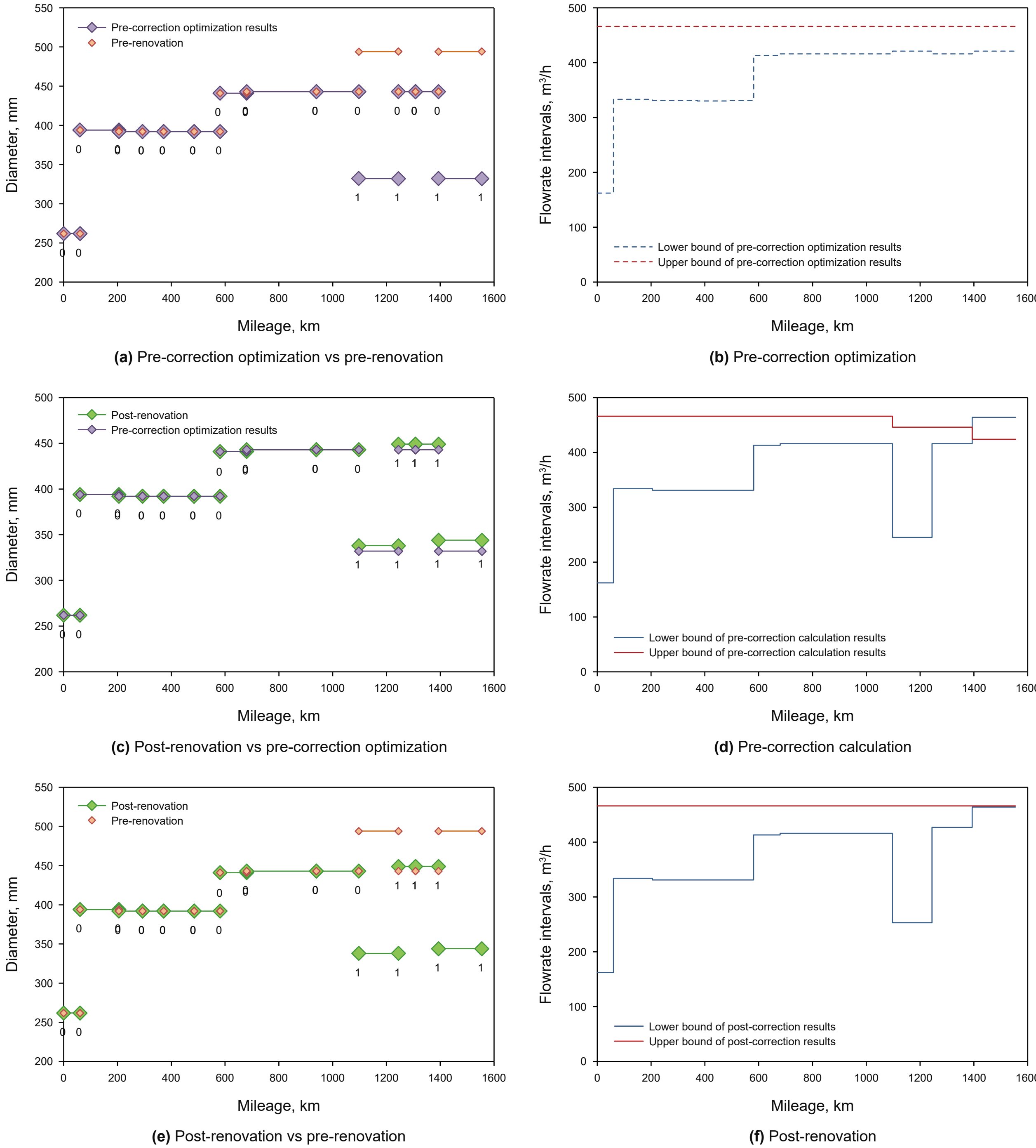

Fig. 7. Diameters and flowrate intervals in non-standardized diameters scenario: **(a)** diameters in pre-correction optimization and pre-renovation; **(b)** flowrate intervals in pre-correction optimization; **(c)** diameters in post-renovation and pre-correction optimization; **(d)** flowrate intervals in pre-correction calculation; **(e)** diameters in post-renovation and pre-renovation; **(f)** flowrate intervals in post-renovation.

Table 7
Economic results and total renovated capacity for standardized diameters scenario.

Stage	Net benefit, 10^4CNY	Transportation revenue, 10^4CNY	Renovation cost, 10^4CNY	Turnover, 10^8t·km	Renovated pipe capacity, 10^4m^3
Pre-renovation	1348.8	1348.8	0	1.4050	0
Pre-correction	1376	1503	127	1.5659	3.1021
Post-correction	1750.0	1878.0	128.0	1.9562	3.0588

$\left(1+fac\right)qp_i^{\max}\Big)$. Then, linear fitting is performed for each small interval, and the slope a_i and intercept b_i are calculated (Eq. (42)).

$$D=\sqrt{\frac{4Q}{\pi v}} \tag{41}$$

$$D_i \approx a_i \mathrm{QP}_i^{\max}+b_i qp_i^{\max} \leq \mathrm{QP}_i^{\max} \leq (1+fac)qp_i^{\max} \tag{42}$$

5. Case study

5.1. Parameter values

The multi-product pipeline in Southwest China is taken as a case study (Fig. 1). The values of general parameters are shown in Table 3, and the pipeline parameters are shown in Table 4. The flowrate intervals of pipe segments after reverse-flow are solved

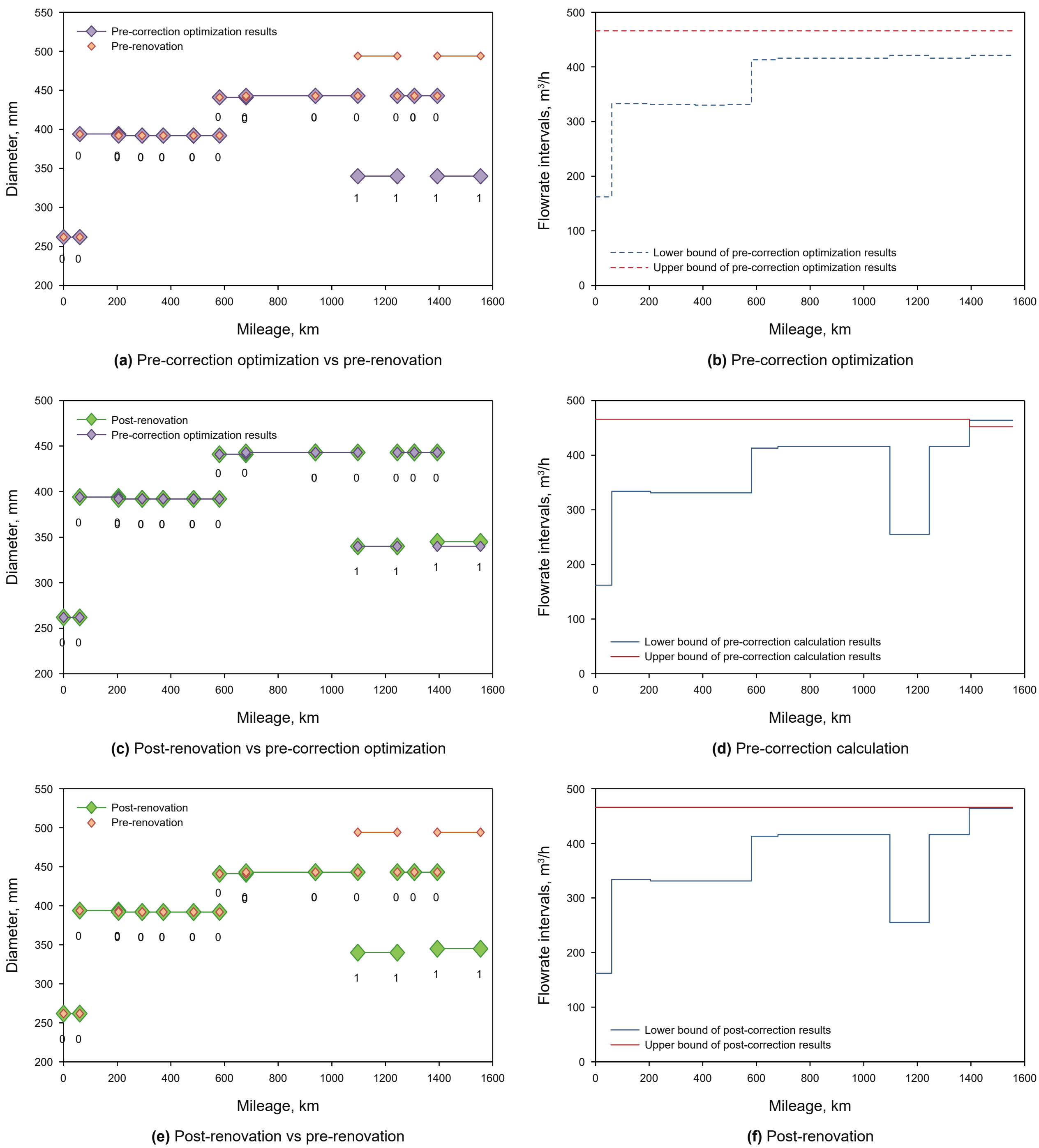

Fig. 8. Diameters and flowrate intervals in standardized diameters scenario: **(a)** diameters in pre-correction optimization and pre-renovation; **(b)** flowrate intervals in pre-correction optimization; **(c)** diameters in post-renovation and pre-correction optimization; **(d)** flowrate intervals in pre-correction calculation; **(e)** diameters in post-renovation and pre-renovation; **(f)** flowrate intervals in post-renovation.

according to calculation criteria in Section 3.1, as shown in Table 5. The flowrate interval of initial station is between 162 m^3/ h and 466 m^3/h.

Table 5 shows the initial values of flowrate intervals obtained by Section 4.1. Columns 2 and 3 present the ultimate values of pipe segment flowrate intervals (Eqs. (9) and (10)). Columns 4 and 5 represent the lower bound defined by Contamination control strategy (Eq. (2)) and MSFC 1 (Eq. (7)) respectively, while columns 6, 7, and 8 represent the upper bound defined by pressure control strategy and flow regime control strategy, MSFC 2 (the first term of Eq. (8)), and MSFC 3 (the second term of Eq. (8)) respectively.

5.2. Result discussion

5.2.1. Scenario of non-standardized diameters

(1) Overall results

The results are categorized into three stages: pre-renovation, pre-correction, and post-correction. The pre-renovation stage corresponds to Module I, while the pre-correction and post-correction stages represent the initial and final iterative results of Modules II and III, respectively. Specifically, pre-correction outcomes are distinguished as optimization results before hydraulic rule verification and calculation results after verification.

For non-standardized diameters, the following parameters are fixed: steel purchase cost of 6000 CNY/t, pipeline transportation price of 0.196 CNY/(t·km), pipeline operating cost at 0.1 CNY/(t·km), 8-year payback period, and 15-day planning horizon. Under these settings, post-renovation total turnover reaches 1.9562×10^8 t·km, which represents a 39.23% increase over pre-renovation levels (Table 6). Net benefit stands at 16.69 million CNY, representing a 23.73% improvement over pre-renovation performance.

(2) Renovation solution

After reverse-flow, if no pipe segments are renovated (abbreviated as pre-renovation), the flowrate interval from the downstream pipe section is an empty set, indicating that oil cannot be transported downstream (Table 5). Taking renovation into account, the optimization result of flowrate interval is an effective set (Fig. 7(b)). At this point, the diameters of both pipe segment $i = 10$ and pipe segment $i = 13$ are reduced, where the inner diameter of pipe segment $i = 10$ is changed from 494 mm to 332 mm, and that of pipe segment $i = 13$ is changed from 494 mm to 332 mm. This measure has successfully expanded the flowrate interval of pipe segments $i = 10$ to $i = 13$, increasing the scope of reverse-flow by 41.69% measured by mileage. However, whether the optimization results satisfy the nonlinear constraints still needs further verification. Specifically, the optimized diameter results DS_i are fed back to Module I of the economic evaluation framework based on the feedback mechanism in Section 2 to recalculate the initial values of the flowrate interval. By comparing the calculation results with the optimization results of the flowrate intervals (Fig. 7(b), (d)), it can be seen that the input of the flowrate interval falls into the categories of upper-limit pessimistic scenario and extremely pessimistic scenario. The specific correction measures are as follows: adjust the diameter of pipe segment $i = 10$ from 332 mm to 338 mm, adjust the diameter of pipe segment $i = 11$ to pipe segment $i = 12$ from 443 mm to 449 mm, and adjust the diameter of pipe segment $i = 13$ from 332 mm to 344 mm (Fig. 7(e)). After correction, the flowrate interval of pipe segment $i = 11$ to pipe segment $i = 13$ is further narrowed, where the upper bound of the recalculated flowrate intervals fully covers the upper bound of optimized flowrate intervals.

Note: (a) The labels 0/1 in subplot indicates whether the pipe segment has been renovated, with 1 indicating yes and 0 indicating no.

5.2.2. Scenario of standardized diameters

(1) Overall results

Taking diameter standardization constraints into account, the transportation revenue and turnover remain unchanged, while

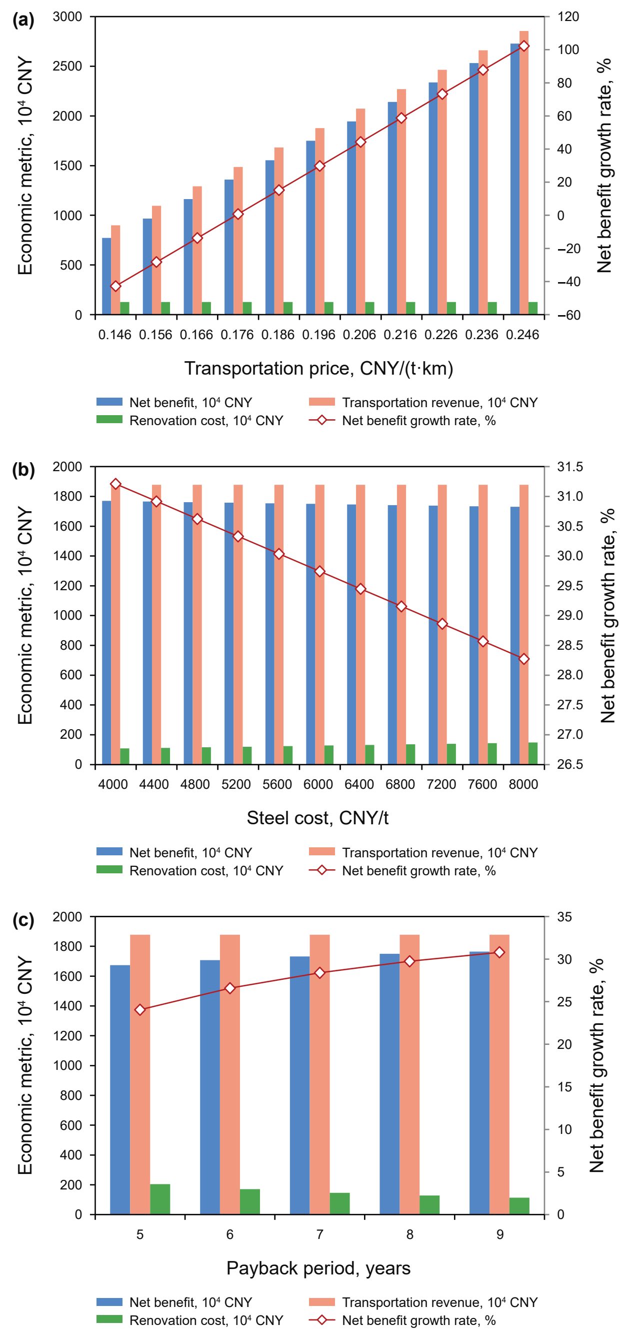

Fig. 9. Impact of economic parameters on economic performance: **(a)** transportation price; **(b)** steel cost; **(c)** payback period.

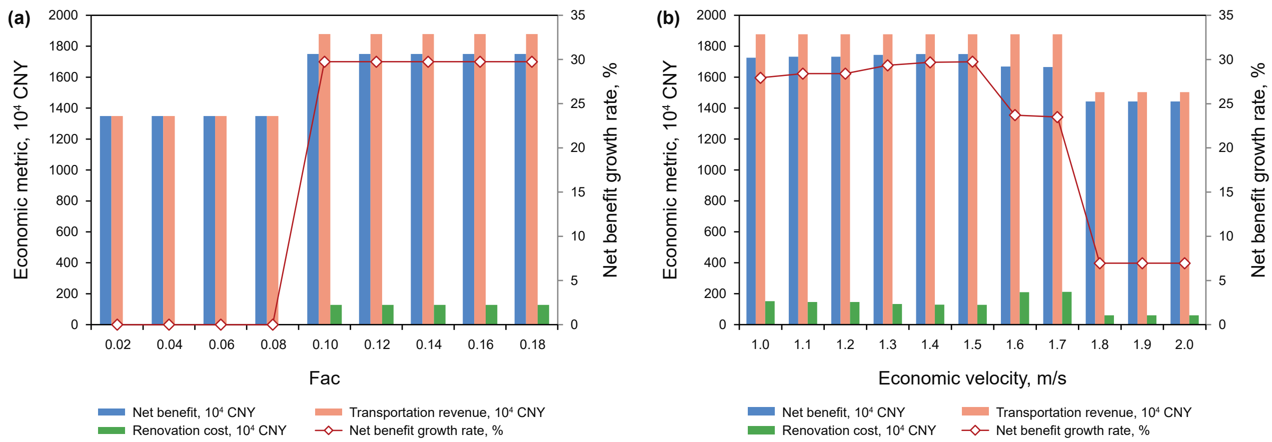

Fig. 10. Impact of model parameters on economic performance: **(a)** fac; **(b)** economic velocity.

renovation cost is reduced. As a result, the net benefit increases by 4.86% compared with non-standardized diameters scenario. Through renovation projects, transport capacity can be increased by 39% measured by total turnover volume (Table 7).

(2) Renovation solution

The optimization results show that after the diameters of pipe segment $i = 10$ and pipe segment $i = 13$ are changed from 494 to 340 mm, pipe segments $i = 10$ to $i = 13$ can continue to transport in reverse-flow (Fig. 8(a) and (b)). By comparing the calculation results with the optimization results of flowrate intervals (Fig. 8(b), (d)), it can be seen that pipe segment $i = 13$ falls into the extremely pessimistic scenario. After the correction procedure is activated, the diameter is adjusted from 340 to 345 mm. At this point, the upper bound of initial calculated flowrate results of pipe segment $i = 13$ can fully cover the upper bound of optimized flowrate results, meaning that the entire pipeline can achieve reverse-flow.

5.2.3. Comparison of the pre-correction and the post-correction

The transportation revenue in the pre-correction stage is 14.97–15.03 million CNY, while the transportation revenue in the post-correction stage is 18.78 million CNY. Compared with pre-correction stage, post-correction stage increases transportation revenue by 19.97%–20.29% by improving turnover volume. The pipe segment $i = 13$ fails to satisfy hydraulic constraints in the pre-correction stage, resulting in a reduction in total turnover. In the post-correction stage, pipe diameters can be effectively adjusted to achieve economic optimization while satisfying the hydraulic constraints along the entire pipeline. The detailed results are shown as Section 5.2.1 and Section 5.2.2.

5.3. Sensitivity analysis of economic benefits

To explore the sensitivity of the economic benefits of renovation project to various influencing factors, this section selects three economic benefit indicators, namely net benefit, transportation revenue and renovation cost, which are used to conduct sensitivity analysis on economic parameters such as unit price of pipeline transportation c^{tran}, unit cost of steel purchase c^{pur}, payback period *pb*, as well as model parameters including flowrate interval expansion factor *fac* and economic velocity v.

The results show that the net benefit has a linear relationship with economic parameters such as unit price of pipeline transportation c^{tran}, unit cost of steel purchase c^{pur}, payback period *pb* (Fig. 9). It is easy to understand that the above three economic parameters only affect the optimization objective in mathematical model, appearing as linear terms in the optimization objective. Among these, the net benefit is particularly sensitive to unit price of pipeline transportation c^{tran}. Taking the pre-renovation net benefit (13.49 million CNY) as the reference indicator, when unit price of pipeline transportation c^{tran} increases from 0.146 CNY/(t·km) to 0.246 CNY/(t·km), the net benefit growth ratio also rises from −42.77% to 102.26%. This paper defines that when post-renovation net benefit is the same as pre-renovation, the parameter at this point is referred to as a "levelized parameter", such as "levelized unit price of pipeline transportation", "levelized unit cost of steel purchase", and "levelized payback period". When "levelized unit price of pipeline transportation" is 0.1755 CNY/(t·km), there is renovation project with a capacity of 30,588 m^3 (Fig. 9 (a)). When unit price of pipeline transportation is higher than the levelized parameter, the implementation of renovation project can not only expand the reverse-flow scale but also achieve growth in economic benefits. By contrast, the impact of unit cost of steel purchase c^{pur} and payback period *pb* on the economic benefits of renovation project is negligible. When unit cost of steel purchase c^{pur} fluctuates within the range of 4000–6000 CNY/t, the net benefit growth ratio remains between 28.28% and 31.21%. When payback period is extended from 5 years to 9 years, the net benefit growth ratio rises from 24.05% to 30.80%. Based on the comprehensive sensitivity analysis results, the renovation project will have certain economic benefits if three economic parameters do not undergo drastic changes.

The impact of model parameters on the economic benefits of renovation project is significantly different from that of economic parameters. The curve of net benefit growth ratio versus flowrate interval expansion factor *fac* shows a stepwise change. The decision results indicate that renovation is not economically viable when *fac* is in [0.02, 0.08], while the net benefit growth ratio stabilizes at 29.74% when *fac* is in [0.1, 0.18] (Fig. 10(a)). The relationship curve between net benefit growth ratio and economic velocity v is the most complex, mainly due to the nonlinear relationship between v and diameter. When the economic velocity increases from 1 m/s to 1.5 m/s, the net benefit growth ratio also rises from 27.93% to 29.74%. As economic velocity v continues to increase, the net benefit growth ratio gradually decreases to 6.96% and then remains unchanged (Fig. 10(b)).

6. Conclusions and future research

Against the backdrop of carbon peaking and neutrality goals, traditional fossil fuel supply schemes demonstrate diminishing efficacy. This paper therefore develops an economic evaluation framework for optimized pipeline flow direction. Given the inadequacy of conventional flowrate intervals and reduced transport capacity under reverse-flow conditions, we propose a framework integrating multi-modal control strategies. Flowrate intervals are recalculated based on pressure regulation, contamination management, and flow regime control. Accounting for pipeline renovation costs, the original mixed-integer nonlinear programming (MINLP) problem is reformulated into a mixed-integer linear programming (MILP) model via piecewise linearization. To improve diameter precision, a physics-based correction module is incorporated. The proposed methodology is validated using a real-world pipeline case study in China. The key findings are as follows.

(1) Through small-scale renovation projects, flowrate intervals of pipeline can be expanded by 41.69% measured by mileage and transport capacity can be increased by 39% measured by total turnover volume.
(2) Compared with the normal rule, the proposed framework increases transportation revenue by 19.97%–20.29% by improving turnover volume.
(3) The net benefit of renovation project is most sensitive to unit price of pipeline transportation. When unit price of pipeline transportation is higher than 0.1755 CNY/ (t·km), the renovation project becomes economically viable. When unit price of pipeline transportation (4000–6000 CNY/t) and payback period (5–9 years) do not fluctuate drastically, the investment can be recovered under premise of small-scale renovation, with the potential for economic benefit growth ranging from approximately 27.93% to 31.21%.
(4) The decision results of renovation scheme are only valuable when model parameters such as the flowrate interval expansion factor (0.1–0.18) and economic velocity (1–1.7 m/s) are within appropriate ranges.

Coordinated flow direction reversal combined with targeted renovations can effectively relieve pipeline congestion and achieve positive returns within a 9-year horizon, while flow optimization alone may lead to infeasible operations. Although sensitivity analysis confirms the economic viability of small-scale projects, large-scale implementation remains cost-intensive and may require policy support. The framework performs well for small-scale to medium-scale systems, but its accuracy deteriorates with increasing scale due to approximation errors (Section 4.3), limiting its applicability to large networks. Future work should focus on defining the applicable scale range and developing scale-adaptive methods to enhance robustness and scalability.

CRediT authorship contribution statement

Ming-Yue Huang: Writing – original draft, Methodology. **Ren-Fu Tu:** Writing – original draft, Conceptualization. **Qi Liao:** Writing – review & editing, Methodology. **Xiao-Meng Bai:** Investigation. **Zheng-Bing Li:** Validation. **You-Yi Liang:** Supervision, Project administration. **Si-Ya Cai:** Investigation. **Yong-Tu Liang:** Visualization.

Declaration of competing interest

The authors declare that they have no known competing financial interests or personal relationships that could have appeared to influence the work reported in this paper.

Acknowledgments

This work was partially supported by the National Natural Science Foundation of China (52202405), the Beijing Natural Science Foundation (4262064) and the Science Foundation of China University of Petroleum, Beijing (2462023BJRC026). The authors are grateful to all study participants.

Nomenclature

Sets/Indices

I	Stations or pipe segments
I^i	Injection stations
I^d	Delivery stations
I^f	The initial injection station
T	Time slots

Variables

BI_t	Binary variable indicating slot t
$BP_{t,i}$	Binary variable indicating pipe segment i is running during slot t
$BD_{t,i}$	Binary variable indicating node i is processing during slot t
DS_i	standard diameter of pipe segment i, mm
QI_i^{max}/QI_i^{min}	Maximum or minimum flowrate at the injection station i, m^3/h
QP_i^{max}/QP_i^{min}	Maximum or minimum flowrate in pipe segment i, m^3/h
RM_i	Auxiliary variable indicating diameter of pipe segment i after renovation, mm
RC_t/LC_t	Right or left coordinate of oil during slot t, m^3
$STA_{i,n}$	Binary variable indicating diameter of pipe segment i is standard diameter n of library
VB_t	volume in pipe of oil during slot t, m^3
$VI_{t,i}$	Product volume at the injection station i during slot t, m^3
$VP_{t,i}$	Product volume flowing through pipe segment i during t, m^3
$VD_{t,i}$	Product volume distributed by station i during slot t, m^3
XE_i	Binary variable indicating maximum and minimum flowrate of pipe segment i has been renovated

Parameters

a_i/b_i	Diameter-flowrate linear fit parameter of pipe segment i
c^{tran}	Unit price of pipeline transportation, CNY/(t·km)
c^{run}	Pipeline operating cost per unit, CNY/(t·km)
c^{pur}	Unit cost of steel purchase, CNY/t
c^{lay}	Laying cost per unit mileage of new pipe section, CNY/(mm·km)
c^{exa}	Excavation cost of old pipe segment, CNY/(mm·km)
c_i^{deal}	Unit distance disposal cost of the old pipe segment, CNY/(mm·km)
c_i^{empty}	Emptying cost of old pipe segment, CNY/(mm·km)

dl_i	Distance of pipe segment i, km
dt	Time interval, h
d_i	Initial diameter of pipe segment i, mm
d_n^{lib}	Standard diameter n of standard pipe diameter library, mm
D_i^{out}	Diameter of pipe segment i, mm
$dp^{\max}$	Maximum permissible pressure drop of segment i, MPa
δ_i	Initial wall thickness of pipe segment i, mm
$\varepsilon_1/\varepsilon_2$	Unit conversion factor
fac	Flowrate interval expansion factor
L_i	Distance of station i from the initial station, km
M/m	Infinite major or minor value
pb	Payback period, years
ρ^{oil}	Density of oil, $\mathrm{kg/m^3}$
ρ^{steel}	Density of steel, $\mathrm{kg/m^3}$
$qi_i^{\max}/qi_i^{\min}$	Initial values of maximum or minimum injection flowrate of station i, $\mathrm{m^3/h}$
$qp_i^{\max}/qp_i^{\min}$	Initial values of maximum or minimum distribution flowrate of pipe segment i under control conditions, $\mathrm{m^3/h}$
$qd_i^{\max}/qd_i^{\min}$	Maximum or minimum distribution flowrate of station i under positive transmission conditions, $\mathrm{m^3/h}$
tl	Planning period, h
vs_i	Coordinate of station i, $\mathrm{m^3}$
v	Economic flowrate, m/s
vc	Pipe capacity, $\mathrm{m^3}$
χ	Cost conversion factor, $\frac{\mathrm{tl}}{350\times24\times\mathrm{pb}}$

References

Acosta-Amado, R.J., 2024. Optimization of petroleum products distribution *via* pipeline systems: Modeling and computational challenges. Heliyon 10 (14), e33947. https://doi.org/10.1016/j.heliyon.2024.e33947.

Cafaro, D.C., Presser, D.J., Grossmann, I.E., 2022. Recent contributions to the optimal design of pipeline networks in the energy industry using mathematical programming. TOP 30 (3), 618–648. https://doi.org/10.1007/s11750-022-00635-3.

Chen, H., Zuo, L., Wu, C., et al., 2017. Optimizing detailed schedules of a multiproduct pipeline by a monolithic MILP formulation. J. Petrol. Sci. Eng. 159, 148–163. https://doi.org/10.1016/j.petrol.2017.09.036.

Garcia-Verdier, T.G., Gutierrez, G., Méndez, C.A., et al., 2024. Optimization of crude oil operations scheduling by applying a two-stage stochastic programming approach with risk management. J. Process Control 133, 103142. https://doi.org/10.1016/j.jprocont.2023.103142.

Herrán, A., de la Cruz, J.M., de Andrés, B., 2010. A mathematical model for planning transportation of multiple petroleum products in a multi-pipeline system. Comput. Chem. Eng. 34 (3), 401–413. https://doi.org/10.1016/j.compchemeng.2009.11.014.

Hou, Z.M., Xiong, Y., Luo, J.S., et al., 2023. International experience of carbon neutrality and prospects of key technologies: Lessons for China. Pet. Sci. 20 (2), 893–909. https://doi.org/10.1016/j.petsci.2023.02.018.

Li, Y., Hu, Z., 2023. MADM-Q, an efficient multi-attribute decision-making support system for offshore decommissioning. Ocean Coast Manag. 243, 106732. https://doi.org/10.1016/j.ocecoaman.2023.106732.

Li, Y., Hu, Z., 2022. A review of multi-attributes decision-making models for offshore oil and gas facilities decommissioning. J. Ocean Eng. Sci. 7 (1), 58–74. https://doi.org/10.1016/j.joes.2021.05.002.

Li, Z., Liang, Y., Ni, W., et al., 2022. Pipesharing: Economic-environmental benefits from transporting biofuels through multiproduct pipelines. Appl. Energy 311, 118684. https://doi.org/10.1016/j.apenergy.2022.118684.

Liao, Q., Liang, Y., Tu, R., et al., 2022. Innovations of carbon-neutral petroleum pipeline: A review. Energy Rep. 8, 13114–13128. https://doi.org/10.1016/j.egyr.2022.09.187.

Liao, Q., Tu, R., Zhang, W., et al., 2023. Auction design for capacity allocation in the petroleum pipeline under fair opening. Energy 264, 126079. https://doi.org/10.1016/j.energy.2022.126079.

Liao, Q., Zhang, H., Xia, T., et al., 2019. A data-driven method for pipeline scheduling optimization. Chem. Eng. Res. Des. 144, 79–94. https://doi.org/10.1016/j.cherd.2019.01.017.

Liao, Q., Zhang, H., Xu, N., et al., 2018. A MILP model based on flowrate database for detailed scheduling of a multi-product pipeline with multiple pump stations. Comput. Chem. Eng. 117, 63–81. https://doi.org/10.1016/j.compchemeng.2018.05.002.

Logsdon, L.B.F., Ferreira Filho, V.J.M., Ribas, P.C., 2025. Optimization models and heuristics for effective pipeline decommissioning planning in the oil and gas industry. Comput. Chem. Eng. 197, 109044. https://doi.org/10.1016/j.compchemeng.2025.109044.

Manafi, B., Sayan, H., 2025. A bi-objective robust optimization and heuristic framework for designing resilient and responsive global supply chains with multimodal transportation. J. Ind. Inf. Integr. 47, 100895. https://doi.org/10.1016/j.jii.2025.100895.

MirHassani, S.A., Ghorbanalizadeh, M., 2008. The multi-product pipeline scheduling system. Comput. Math. Appl. 56 (4), 891–897. https://doi.org/10.1016/j.camwa.2008.01.035.

Qiu, R., Liang, Y.T., Liao, Q., et al., 2022. Primary logistics planning of oil products under the imbalance of supply and demand. Pet. Sci. 19 (4), 1915–1925. https://doi.org/10.1016/j.petsci.2022.03.021.

Ramos Rosa, V., Camponogara, E., Martins Ferreira Filho, V.J., 2018. Design optimization of oilfield subsea infrastructures with manifold placement and pipeline layout. Comput. Chem. Eng. 108, 163–178. https://doi.org/10.1016/j.compchemeng.2017.08.009.

Raoni, R., Secchi, A.R., Biscaia Jr., E.C., 2017. Novel method for looped pipeline network resolution. Comput. Chem. Eng. 96, 169–182. https://doi.org/10.1016/j.compchemeng.2016.10.001.

Sandana, D., Gallon, N., Burkinshaw, O., et al., 2022. Safe repurposing of vintage pipelines for hydrogen in North America. In: 2022 14th International Pipeline Conference. https://doi.org/10.1115/IPC2022-87088.

Sidki, M., Tchernev, N., Féniès, P., et al., 2025. Multiproduct pipeline scheduling: A comprehensive bibliometric analysis and a systematic literature review. Comput. Chem. Eng. 192, 108911. https://doi.org/10.1016/j.compchemeng.2024.108911.

Spezakis, Z., Xydis, G., 2023. Transporting offshore wind power in the Western Gulf of Mexico: retrofitting existing assets for power transmission *via* green hydrogen: A review. Environ. Sci. Pollut. Res. 30 (44), 99088–99099. https://doi.org/10.1007/s11356-022-23292-2.

Thompson, D.J., Farid, A.M., 2023. A reference architecture for the American multi-Modal Energy System enterprise. J. Ind. Inf. Integr. 36, 100521. https://doi.org/10.1016/j.jii.2023.100521.

Tu, R., Liao, Q., Huang, L., et al., 2023a. Pipeline sharing: remaining capacity estimation of multiproduct pipelines. Chem. Eng. Res. Des. 191, 338–352. https://doi.org/10.1016/j.cherd.2023.01.028.

Tu, R., Liao, Q., Xu, N., et al., 2023b. Pipeline sharing: potential capacity analysis of biofuel transportation through existing pipelines. J. Clean. Prod. 398, 136507. https://doi.org/10.1016/j.jclepro.2023.136507.

Tu, R., Liu, C., Shao, Q., et al., 2024. Pipeline sharing: optimal design of downstream green ammonia supply systems integrating with multi-product pipelines. Renew. Energy 223, 120024. https://doi.org/10.1016/j.renene.2024.120024.

Wang, B., Yuan, M., Yan, Y., et al., 2019a. Optimal design of an oil pipeline with a large-slope section. Eng. Optim. 51 (9), 1480–1494. https://doi.org/10.1080/0305215X.2018.1525710.

Wang, B., Zhang, H., Yuan, M., et al., 2019b. Sustainable crude oil transportation: design optimization for pipelines considering thermal and hydraulic energy consumption. Chem. Eng. Res. Des. 151, 23–39. https://doi.org/10.1016/j.cherd.2019.07.034.

Xu, N., Liao, Q., Li, Z., et al., 2021. An efficient decomposition approach for the low-energy scheduling of a straight multiproduct pipeline. Chem. Eng. Res. Des. 165, 341–360. https://doi.org/10.1016/j.cherd.2020.10.022.

Zhang, Q., Liu, J.F., Gao, Z.H., et al., 2023. Review on the challenges and strategies in oil and gas industry's transition towards carbon neutrality in China. Pet. Sci. 20 (6), 3931–3944. https://doi.org/10.1016/j.petsci.2023.06.004.

Zhou, X., van Gelder, P.H.A.J.M., Liang, Y., et al., 2020a. An integrated methodology for the supply reliability analysis of multi-product pipeline systems under pumps failure. Reliab. Eng. Syst. Saf. 204, 107185. https://doi.org/10.1016/j.ress.2020.107185.

Zhou, X., Zhang, H., Qiu, R., et al., 2019. A two-stage stochastic programming model for the optimal planning of a coal-to-liquids supply chain under demand uncertainty. J. Clean. Prod. 228, 10–28. https://doi.org/10.1016/j.jclepro.2019.04.264.

Zhou, X., Zhang, H., Xin, S., et al., 2020b. Future scenario of China's downstream oil supply chain: low carbon-oriented optimization for the design of planned multi-product pipelines. J. Clean. Prod. 244, 118866. https://doi.org/10.1016/j.jclepro.2019.118866.